Hydrol. Earth Syst. Sci. Discuss., 7, 3129–3157, 2010
www.hydrol-earth-syst-sci-discuss.net/7/3129/2010/
doi:10.5194/hessd-7-3129-2010

Hydrology and Earth System Sciences Discussions

Uncertainty in the impacts of projected climate change on the hydrology of a subarctic environment: Liard River Basin

R. Thorne

School of Geography and Earth Sciences, McMaster University, Hamilton, Ontario, Canada

Received: 30 April 2010 – Accepted: 5 May 2010 – Published: 21 May 2010

Correspondence to: R. Thorne (thornerf@mcmaster.ca)

Published by Copernicus Publications on behalf of the European Geosciences Union.

Abstract

Freshwater inputs from the Mackenzie River into the Arctic Ocean contribute to the control of oceanic dynamics and sea ice cover duration. Half of the annual runoff from the Mackenzie River drains from mountainous regions, where the Liard River, with a drainage area of 275 000 km^2, is especially influential. The impact of projected atmospheric warming on the discharge of the Liard River is unclear. Here, uncertainty in climate projections associated with GCM structure (2 °C prescribed warming) and magnitude of increases in global mean air temperature (1 to 6 °C) on the river discharge are assessed using SLURP, a well-tested hydrological model. Most climate projections indicate (1) warming in this subarctic environment that is greater than the global mean and (2) an increase in precipitation across the basin. These changes lead to an earlier spring freshet (1 to 12 days earlier), a decrease in summer runoff (up to 22%) due to enhanced evaporation, and an increase in autumn flow (up to 48%), leading to higher annual discharge and more freshwater input from the Liard River to the Arctic Ocean. All simulations project that the subarctic nival regime will be preserved in the future but the magnitude of changes in river discharge is highly uncertain (ranging from a decrease of 3% to an increase of 15% in annual runoff), due to differences in GCM projections of basin-wide temperature and precipitation.

1 Introduction

A quantitative understanding of the runoff response of subarctic rivers to climate change and variability is important for planning and development, environmental conservation, social well-being and the livelihood of communities on valleys and flood plains. The Mackenzie River is the largest river in North America that brings freshwater from the subarctic and Arctic environments in Canada to the Arctic Ocean. Current climate projections from General Circulation Models (GCMs) indicate preferential warming of this region, relative to the global mean, which can have substantial secondary

HESSD

7, 3129–3157, 2010

impacts on the environment (Bonsal and Kochtubajda, 2009). Freshwater input to the Arctic Ocean from the Mackenzie River forms a surface layer on the denser saline seawater that allows the formation of sea ice. The extent and duration of sea ice cover, in turn, affects affects oceanic evaporation and, hence, moisture and heat fluxes into the Arctic atmosphere. Changes in freshwater inputs to the Arctic Ocean therefore have global climatic implications beyond the drainage basins from which the water is derived.

The Mackenzie River receives half of its annual runoff from mountainous regions that occupies less than one third of the total basin area, and most of this flow is produced in the spring (Woo and Thorne, 2003). The mountainous Liard Basin, an area that has experienced warming in recent decades (Zhang et al., 2000), is a major tributary of the Mackenzie River. Rivers in the Liard Basin are not regulated and the hydrometeorological records permit the assessment of flow responses to changes in climatic conditions without the need to consider human interferences. Owing to the sparse population in the vast domain of northern Canada, climatic and hydrometric data are scarce. In this study, gridded climate observations and projections are applied to a macro-scale hydrological model to quantify changes in the magnitude and timing of the discharge of the Liard River. Following calibration, the hydrological model is forced with a range of climate change scenarios, designed to allow the investigation of uncertainty between different GCMs and climate sensitivities. The scenarios explored herein will permit an investigation of the impacts of specific thresholds of climate change on the quantity and seasonality of water resources in the Liard Basin.

2 Study area

The Liard River Basin drains an area of 275 000 km^2 and is a typical large mountainous catchment in the Western Cordillera (Fig. 1). The Cordillera is effective in blocking most moisture-bearing winds from the Pacific Ocean and orographic precipitation is most notable in the western sector. Snow is a major form of precipitation, but rainfall

HESSD
7, 3129–3157, 2010

is common in summer and autumn. Located at higher latitudes (57–63° N), the basin has a cold temperate to subarctic setting. There is also strong vertical zonation in the mountain climate, but most of the weather stations are located in the valleys. Land cover in the basin is largely comprised of tundra, and both deciduous and evergreen forests. The Liard River is gauged at its mouth (at Fort Simpson, 61°44′49″ N and 121°13′25″ W), above the confluence with the Mackenzie River. Discharge data from this gauging station are used for calibration and for comparison with values simulated by the hydrological model.

3 Hydrological model

For hydrological simulations, the SLURP (Semi-distributed Land-use-based Runoff Processes) model (version 12.2) is used as it has been well tested in mountainous basins (Kite et al., 1994). SLURP divides a large catchment into aggregated simulation areas (ASAs). Each ASA encompasses a number of land cover types characterised by a set of parameters. Simulations using SLURP are based on: (1) a vertical component consisting of daily surface water balance and flow generation from several storages; and (2) a horizontal component of flow delivery within each ASA and channel routing to the basin outlet. The present study subdivides the Liard Basin into 35 ASAs (Fig. 2) which partitions the basin into distinctive sub-basins. Mean elevation, area and areal percentages occupied by each land cover type are estimated from digital elevation data combined with a land cover map. The hydrological model was calibrated with the gauged station at the mouth of the Liard River at Fort Simpson from 1973 to 1990 (Fig. 3) using gridded (0.5° × 0.5°) climate observations, CRU TS3.0 (Mitchell and Jones, 2005; http://badc.nerc.ac.uk/data/cru/). The designated parameters and procedures used in the calibration were the same as described in Thorne and Woo (2006) and Woo and Thorne (2006). The calibration yielded a Nash-Sutcliffe statistic (Nash and Sutcliffe, 1970) of 0.75 and a root-mean-square error of 1347 $m^3 s^{-1}$ or a normalized root-mean-squared error of 8%. The calibration period shows a good fit to the observed discharge.

HESSD
7, 3129–3157, 2010

4 Data and methods

In this study, future climate scenarios for temperature and precipitation were generated using the ClimGen pattern-scaling technique described in Todd et al. (2010). Scenarios were generated for a prescribed warming of a global mean temperature of 1, 2, 3, 4, 5, and 6 °C using the UKMO HadCM3 GCM, and for a 2 °C global mean warming with six additional GCMs: CCCMA CGCM31, CSIRO Mk30, IPSL CM4, MPI ECHAM5, NCAR CCSM30, and UKMO HadGEM1. The scenarios cover a 30-year period from 2040 to 2069, using the 1961 to 1990 record as the baseline for this study. Year-to-year variability was excluded in the analysis of hydrological changes in the basin. The simulations assumed no change in land cover and soil conditions under a natural setting.

To generate the required daily climate data for the model (precipitation, mean and minimum temperature), gridded ($0.5^\circ \times 0.5^\circ$) monthly observations (CRU TS3.0) and climate projections (ClimGen) were transformed using a stochastic weather generator (Kilsby et al., 2007). The weather generator was conditioned using climate station data statistics within and around the Liard Basin. These include: the coefficient of variation of daily precipitation (on days when rain occurs) and the standard deviation of daily temperature (after the seasonal cycle in temperature has been removed). The baseline dataset spans the period 1961 to 1990 during which the quality of the data generally increases towards the latter part of the time period as more station data became available. Although there are errors associated with the application of gridded, global-scale datasets, discrepancies most likely occur where the historical meteorological observations are sparse. The temperature and precipitation distribution across the basin is examined, in addition to the monthly discharge hydrograph produced by each future scenario. The first day of prominent hydrograph rise is also examined following the methodology by Burn (2008). To simplify the analysis of both temperature and precipitation, four seasons were examined: winter (December to February), spring (March to May), summer (June to August) and autumn (September to November).

5 Climate variables

5.1 Spatial distribution of temperature and precipitation

Spatial variations in temperature and precipitation changes associated with each scenario were mapped over the Liard Basin (Fig. 4). The maps show the 30-year mean of each season for the CRU TS3.0 data and aid in analyzing how river discharge is affected by specific changes in temperature and precipitation. Temperatures are generally warmer in the southeast and decrease northwest towards high latitude and higher elevation. Precipitation in the mountainous basin is significantly correlated with altitude and latitude, increasing with proximity to the Pacific Ocean but decreasing northeastward (Woo and Thorne, 2006). In the winter season, snowfall is highest at the southwestern corner of the basin, while the eastern sector lies to the lee of the prevailing westerlies and generally has low winter precipitation. For the spring, heavier precipitation is seen in the southeastern corner of the basin. Summer produces the largest precipitation in all of the seasons, while autumn rainfall varies across the basin.

5.2 Uncertainty in projected changes in air temperature

With the spatial pattern of temperature and precipitation previously discussed, spatial variations brought about by each climate change scenario are discussed. Spatial temperature changes in each season by the scenarios are shown in Fig. 5a. For the winter season, CCCMA shows a 4–6 °C increase in the north and a 2–4 °C increase in the south, with a similar pattern produced by HadGEM1 with a large increase of 4–6 °C in the northeast and a 2–4 °C increase in the southwest. A similar pattern of warming though lower in magnitude is projected under the HadCM3 scenario, with a 2–4 °C increase in the north and a 0–2 °C increase in the south. The CSIRO, IPSL and NCAR scenarios have a basin wide increase of 2–4 °C, whereas MPI has a basin wide increase of 4–6 °C. In the spring, the CCCMA, HadCM3 and NCAR scenarios have a basin wide increase of 0–2 °C, with a warmer increase of 2–4 °C for the CSIRO, IPSL

HESSD
7, 3129–3157, 2010

and MPI scenarios. HadGEM1 has a 2–4 °C increase in the north, with a 0–2 °C increase in the south. In the summer, a larger increase is found in the lowlands in the northeast, and a smaller increase along the mountain range in the west for CCCMA, with a reversed pattern for NCAR. CSIRO has an increase of 0–2 °C over the Liard, with the remaining scenarios showing a basin wide increase of 2–4 °C. For the autumn season, each scenario has a 2–4 °C increase across the basin, with the exception of CSIRO, with only an increase of 0–2 °C.

Common to all scenarios is an increase of air temperature for all seasons, in some cases with a variation of only 1 °C between the scenarios. However, even a 1 °C temperature difference would impact the evaporation and freeze/melt rates within the basin. Winter has the largest range of projected warming, with 0–2 °C warming by HadCM3 to the largest increase, up to 6 °C, for CCCMA, MPI and HadGEM1. On an annual basis, the highest projected temperature changes were by the MPI and IPSL scenarios. Most climate projections suggest a warming temperature in the Liard Basin greater than the global prescribed warming theme of 2 °C.

With the steady global temperature increase in the HadCM3 scenarios (Fig. 5b); there is a 0–2 °C change in the basin for each season in the 1 °C scenario, which increases to 2–4 °C for the summer and fall seasons at the 2 °C scenario. The basin becomes much warmer in the winter with the 3 °C scenario. From the 4 °C to the 6 °C warming scenarios, the winter season is warming more in the north than in the south, with the warmest (6–8 °C) increase with the 6 °C warming scenario. A slight increase is seen during the spring, with the 6 °C scenario causing a 4–6 °C rise in the northern and southern portions of the basin. The summer season has the largest increase of the seasons, with an 8–10 °C increase in the warmest scenario. The fall season also increases steadily ranging from 4–6 °C to 6–8 °C across the basin.

5.3 Uncertainty in projected changes in precipitation

The change in precipitation in the Liard Basin projected by the climate change scenarios are shown in Fig. 6a. Precipitation projections for all seasons vary greatly by

HESSD
7, 3129–3157, 2010

location and magnitude for each season, unlike the projections for temperature. In the winter season, most scenarios project the largest increase of precipitation in the western sector of the basin, although the magnitude varies with each scenario. The largest increases (over 30 mm) are projected by CCCMA and HadCM3 in the west, which decrease eastward. CSIRO projects very little change in winter precipitation across the basin. IPSL projects little change in the north, but up to 20 mm more precipitation across the rest of the basin. MPI, NCAR and HadGEM1 scenarios have similar projections, with approximately a 20 mm increase in the west and little change in the east.

Spatial patterns between the scenarios for the spring season are quite different. CCCMA and HadGEM1 scenarios show a basin wide increase of 10–20 mm, whereas the CSIRO and HadCM3 scenarios show an increase of 10–20 mm in the southeast sector and a small increase for the rest of the basin. The MPI scenario shows an increase of 10–20 mm in the west and little change in the east. An opposite pattern is projected by NCAR. Finally the IPSL scenario shows a small increase in the west, but a decrease in the eastern sector.

Projections of summer precipitation by the scenarios differ greatly from each other. CCCMA has an increase of up to 40 mm in the eastern sector, with an increase of up to 30 mm in the west. An increase of up to 20 mm is projected for the central part of the Liard for the CSIRO scenario. Both IPSL and MPI scenarios project a decrease in the east, with increasing rainfall in the west. The HadCM3 scenario has a large increase in the northwestern and southeastern parts of the basin. NCAR projects a basin wide increase of 20–40 mm, while HadGEM1 shows a decrease or little change across the basin.

A variety of patterns continue over from the summer into the autumn season. The CCCMA scenario increases up to 30 mm in the northwestern and southeastern parts of the basin, with an increase of 20 mm in between. Basin wide increases of up to 20 mm are projected for both CSIRO and NCAR scenarios. IPSL shows little increase in the northeast and up to 20 mm more precipitation in the southwest. HadCM3 ranges

HESSD
7, 3129–3157, 2010

from 30 mm in the east, decreasing west, similar to the patterns projected by MPI and HadGEM1, although HadGEM1 shows a lower increase in precipitation.

Annual precipitation values from each scenario show the CCCMA and MPI scenarios with the largest increase, and CSIRO, IPSL and HadGEM1 with the lowest basin wide increase. For the steadily warming HadCM3 scenarios (Fig. 6b), as the temperature increases in the basin, precipitation also increases. For each season, a common pattern is a large increase of precipitation in the north, with a small increase in the south, except for spring when a reverse pattern occurs. For the 1 °C scenario, the autumn and winter seasons have the largest increase in precipitation, with little change in spring and summer. As the scenario temperature increases, basin wide precipitation increases by at least 10 mm, except in the summer, where precipitation only increases in the northwest sector.

5.4 Summary of projected temperature and precipitation

By examining the spatial patterns in projected changes to both temperature and precipitation by each scenario, some general patterns emerge. Most scenarios project an increase of temperature, with the largest increase found in the winter season. However, such a temperature increase in the winter would be inconsequential compared to the impact on thermal and hydrological activities that occur in other seasons (e.g. freeze/melt rates, increased evaporation). The MPI and IPSL scenarios had the highest annual increase of temperature. The most noticeable increases occur in the warming HadCM3 scenarios. Here, as the global temperature steadily increases, the summer and fall seasons receive the largest warming, expected to enhance evaporation over the basin. Despite the lowest temperature increase in the spring, the effect is stronger with expected earlier snowmelt and river ice break-up.

Precipitation projections generally show an increase in the Liard Basin, but these projections vary greatly spatially and by magnitude depending on the scenario. IPSL and HadGEM1 scenarios actually project decreased precipitation in some areas. With each degree of warming for the HadCM3 scenarios, precipitation increases by at least 10 mm.

HESSD
7, 3129–3157, 2010

Uncertainty in the climate patterns and magnitude will have a pronounced impact on the simulated hydrographs produced by each climate change scenario. Temperature increases will affect freeze/melt and evaporation rates, but the uncertainty created by the mix of scenarios will give rise to different rates, and range of projected hydrographs. Precipitation is shown to have more uncertainty between the different scenarios, both spatially and in magnitude, when compared to temperature. This will have profound effects on peak flow due to snowmelt and summer secondary peaks due to rainfall.

5.5 Climate projections compared to previous studies

The temperature and precipitation projections for the Liard Basin described above are comparable to previous studies in the area. Woo et al. (2008) examined the response of the Liard River to climate change projected by the CCCMA under the more conservative B2 emissions scenario. Their study suggests warming across the basin, especially in the winter and spring seasons. However, precipitation is projected to decrease in the winter and increase in the spring, with little change during the summer and autumn seasons. Bonsal and Kochtubajda (2009) examined temperature and precipitation projections from 18 future scenarios over the Beaufort Sea and Mackenzie Delta on annual and seasonal scales. Although further north than the Liard Basin, their study showed similar results, with temperature, and for the most part precipitation increasing, but with considerable range on both temporal and spatial scales. Seasonal temperature increases were larger in the autumn and winter, similar to projections for the Liard. Winter and spring precipitation has the greatest percentage change, with some regional decreases, particularly in spring and autumn. Decreases of precipitation in the Liard Basin are only observed during the spring and summer seasons by two scenarios (IPSL and HadGEM1). Notably mentioned is the high degree of uncertainty found with respect to future climate over the Arctic region, similar to the findings in the Liard Basin. Kattsov et al. (2007), with the use of atmosphere-ocean general circulation models, found that precipitation over the Mackenzie Basin increases through the twenty-first century, with the largest increase in winter and fall. The river discharge into

HESSD
7, 3129–3157, 2010

the Arctic Ocean is projected to increase by all scenarios. Similar results were found by Nohara et al. (2006), with an increase in precipitation leading to an increase in discharge from the Mackenzie Basin projected by 19 coupled atmosphere-ocean general circulation models based on the SRES A1B scenario. Peak timing in the Mackenzie River is projected to occur earlier due to earlier snowmelt caused by the warming.

6 Streamflow

6.1 Changes in the basin water balance

After running the hydrological model using climate data as input from each scenario, components of the water balance were calculated for the whole basin. Table 1 shows baseline averages for the 30-year period (2040 to 2069) and percent difference from future scenarios of precipitation, evaporation and computed runoff. Compared to baseline values, all scenarios project an increase in precipitation (6 to 18%) and evaporation (12 to 30%). However, average computed runoff yielded different results, with most scenarios showing an increase of 4 to 15%. The HadGEM1 scenario simulates a similar amount of annual runoff, and the IPSL scenario generates a loss of 3%. With each degree of warming under the HadCM3 GCM, each water balance component increases by at least 5%, with the exception of evaporation where there is a jump of 11% between the 2 °C and 3 °C scenarios.

Discrepancies in water balance components between scenarios can be attributed to the differences in projected precipitation and temperature. An example can be seen with computed runoff between the IPSL, MPI and HadGEM1 scenarios. Both the IPSL and MPI scenarios have higher annual temperature increases, but the MPI scenario has a much larger increase in precipitation compared with IPSL. This explains the higher average precipitation and positive computed runoff despite an elevated evaporation rate. The HadGEM1 scenario has an increase of both precipitation (despite a decrease in summer rainfall) and temperature, where the increased precipitation and

HESSD
7, 3129–3157, 2010

possibly more snowmelt is offset by a higher evaporation rate, producing no change in the annual computed runoff. Compared to the HadGEM1 scenario, the decrease in simulated runoff by IPSL, despite both scenarios having similar increases of precipitation, can be attributed to a higher evaporation rate or lost of runoff to storage. Examination of the hydrographs by each scenario compared to the baseline permits further clarification.

6.2 Projected changes in intra-annual river discharge

To investigate changes in the streamflow response brought on by the future scenarios, hydrologic simulations were performed and the results were averaged into monthly intervals for the 30-year period with differences in the first day of prominent hydrograph rise and seasonal runoff presented in Table 2. The Liard River has a typical subarctic nival regime, in which snowmelt dominates, generating annual high flows in combination with summer rainfall (Woo and Thorne, 2003). Autumn rainfall gives rise to a secondary peak that is lower in magnitude than the spring flood.

Monthly hydrographs simulated using the 2 °C prescribed warming scenarios (Fig. 7) indicate an alteration to the hydrological regime and magnitude of discharge to the Liard River. A notable feature is the increase of winter low flow for all scenarios (3 to 8%) due to the higher recession flow from the larger autumn rainfall events. Warmer spring temperatures lead to an earlier arrival of snowmelt runoff advancing the starting date of the spring freshet by 1 to 12 days. The MPI and IPSL scenarios have the highest spring runoff and earliest date of hydrograph rise as a result of higher projected temperatures for the spring season (Sect. 4.2). With the increased precipitation in the winter and spring for most scenarios, the high flows (with increases of 16 to 36%) continue into the summer. An earlier melt season and increase in winter snow accumulation can extend the basin snowmelt over a longer period. An early melt year depletes the snow gradually so that runoff becomes less concentrated (Woo and Thorne, 2006).

Beyond the spring flow, the MPI, IPSL and HADGEM1 scenarios (higher temperatures in the summer, an increase in winter snowfall, and spring and summer precipitation lower than the baseline) result in a lower peak flow, or in the case of the HADGEM1 scenario, a similar peak flow compared to the baseline. The IPSL scenario projects the primary peak flow to occur a month earlier. The CCCMA and HadCM3 scenarios both have the highest peak flow. Summer flow from the scenarios, with the exception of a 9% increase by CCCMA, is projected to be lower than the baseline, with a loss up to 22%. For these scenarios, an increase in summer rainfall does not compensate for an increase in evaporation created by high temperatures. The autumn months show an increase in the secondary peak for all scenarios (1 to 24%). In these months, the evaporation rate is low and an increase in precipitation is projected. The highest flow is generated by MPI, which also has the largest increase in autumn precipitation.

The impact of prescribed increases with the HadCM3 scenarios on the discharge of the Liard River (Fig. 8) shows similar findings. As the temperature warms, discharge increases from autumn to spring months due to an increase in precipitation, with the largest increase in spring (up to 75%, Table 2). An increase in evaporation balanced by an increase in precipitation creates little change in total summer runoff. The autumn secondary peak is enhanced with each degree of warming (up to 48%).

Differences in temperature and precipitation between the scenarios are shown to affect simulated hydrographs in terms of timing and magnitude of the hydrological regime. Even a higher temperature increase by the MPI and IPSL scenarios have shown to advance the starting date of the spring freshet. Precipitation variations also have significant impacts on the regime, where increases in precipitation contribute to increased discharge by snowmelt or rainfall. A temperature increase combined with precipitation decrease in summer shows a different result by the IPSL scenario (Fig. 7).

The subarctic nival regime will be preserved in the Liard River and winter and spring flow will increase with an earlier rise in spring freshet. The timing of primary and secondary peaks is maintained, with the exception of IPSL. Summer flow will decrease, but will be balanced by an increase in the fall. However, the discharge magnitude

HESSD
7, 3129–3157, 2010

differs between the scenarios, continuing into the summer and autumn months. This uncertainty in projected temperature and precipitation by the 2 °C prescribed warming scenarios will create discrepancies with regards to projections of river discharge.

7 Conclusions

Like many high latitude areas, the mountainous region of subarctic Canada has experienced recent warming and it is an area of large inter-annual temperature variations, notably in winter. Quantifying how climate tendencies affect streamflow, especially in the spring melt season, is critical not only to regional water resource management but to understanding the influence of freshwater on the Arctic sea-ice cover and global climate system. The scarcity of climate stations in the remote region prevents a comprehensive appraisal of climatic influences on discharge, but results from global gridded observations (CRU TS3.0) and projections permit the analysis through the availability of spatial information.

This study assesses uncertainty in climate projections for (1) 2 °C prescribed increase in global mean air temperature from seven GCMs and (2) scaled increases in global mean air temperature of 1 to 6 °C using the HadCM3 GCM. Hydrological modelling was used to simulate the effects of climate change on streamflow. The case study of the Liard River suggests that, in the absence of major land-use changes in the basin, river discharge will be impacted by atmospheric warming greater than the global mean, which produces earlier melt and increased evaporation. All scenarios indicate that the subarctic nival regime will be preserved in the future, but with a shift towards an earlier rise in spring runoff (1 to 12 days earlier). These streamflow projections are similar to the study by Woo et al. (2008). However, the magnitude of change in the discharge has a high degree of uncertainty due to projected differences in the increase of temperature and precipitation within the basin, ranging from a decrease of 3% to an increase of 15% in annual runoff. These uncertainties are confirmed by Kattsov et al. (2007) and Nohara et al. (2006) for the Mackenzie River Basin.

HESSD
7, 3129–3157, 2010

Freshwater contribution to the Mackenzie River (and subsequently the Arctic Ocean) from the Liard Basin will generally increase, which can have an impact on the sea ice cover and Arctic atmosphere. An increase in freshwater discharge will reduce sea ice volume and thereby potentially reduce thermohaline circulation (Rennermalm et al., 2006).

Current studies on trends and variability in the Liard Basin (Abdul Aziz and Burn, 2006; Burn, 2008; Burn et al., 2004; Woo et al., 2008) indicate that the results projected by the climate scenarios are feasible since historical records indicate an increase in winter flow, an earlier onset of spring runoff due to increasing trends in temperature, and a summer flow decrease related to more frequent warm summers, that leads to greater evaporation. Uncertainty in the current projections of the impacts of climate change in the Liard River presents an indication of projected changes in the quantity and seasonality of water resources. Reducing uncertainty associated with the scenarios is problematic without adequate ground-based measurements. Instead, to help with projections in an area sensitive to climate forcing, hydrometeorological monitoring networks must be maintained, and even intensified.

Acknowledgements. Climate scenarios and support for this research were facilitated by a grant from the UK Natural and Environmental Research Council (NERC), under the Quantifying and Understanding the Earth System (QUEST) programme (Ref. NE/E001890/1). I am most appreciative of the helpful comments from Ming-ko Woo, Richard Taylor and various reviewers.

References

Abdul Aziz, O. I. and Burn, D. H.: Trends and variability in the hydrological regime of the Mackenzie River Basin, J. Hydrol., 319, 282–294, 2006.

Bonsal, B. R. and Kochtubajda, B.: An assessment of present and future climate in the Mackenzie Delta and the near-shore Beaufort Sea region of Canada, Int. J. Climatol., 29, 1780–1795, 2009.

Burn, D. H.: Climatic influences on streamflow timing in the headwaters of the Mackenzie River Basin, J. Hydrol., 352, 225–238, 2008.

Burn, D. H., Cunderlik, J. M., and Pietroniro, A.: Hydrological trends and variability in the Liard River basin, Hydrol. Sci. J., 49, 53–67, 2004.

Kattsov, V. M., Walsh, J. E., Chapman, W. L., Govorkova, V. A., Pavlova, T. V., and Zhang, X.: Simulation and projection of Arctic freshwater budget components by the IPCC AR4 global climate models, J. Hydrometeorol., 8(3), 571–589, 2007.

Kilsby, C. G., Jones, P. D., Burton, A., Ford, A. C., Fowler, H. J., Harpham, C., James, P., Smith, A., and Wilby, R. L.: A daily weather generator for use in climate change studies, Environ. Modell. Softw., 22, 1705–1719, 2007.

Kite, G. W., Dalton, A., and Dion, A.: Simulation of streamflow in a macroscale watershed using general circulation model data, Water Resour. Res., 30, 1547–1559, 1994.

Mitchell, T. D. and Jones, P. D.: An improved method of constructing a database of monthly climate observations and associated high-resolution grids, Int. J. Climatol., 25, 693–712, 2005.

Nash, J. E. and Sutcliffe, J. V.: River flow forecasting through conceptual models: Part 1 – a discussion of principles, J. Hydrol., 10, 282–290, 1970.

Nohara, D., Kitoh, A., Hosaka, M., and Oki, T.: Impact on climate change on river discharge projected by multimodel ensemble, J. Hydrometeorol., 7(5), 1076–1089, 2006.

Rennermalm, A. K., Wood, E. F., Déry, S. J., Weaver, A. J., and Eby, M.: Sensitivity of the thermohaline circulation to Arctic Ocean runoff, Geophys. Res. Lett., 33, L12703, doi:10.1029/2006GL026124, 2006.

Thorne, R. and Woo, M. K.: Efficacy of a hydrologic model in simulation discharge from a large mountainous catchment, J. Hydrol., 330, 301–312, 2006.

Todd, M. C., Osborn, T., and Taylor, R. G.: Quantifying uncertainty in the impact of climate change on water resources at river basin and global scales – a unified approach, Hydrol. Earth Syst. Sci. Discuss., in preparation, 2010.

Woo, M. K. and Thorne, R.: Streamflow in the Mackenzie Basin, Canada, Arctic, 56(4), 328–340, 2003.

Woo, M. K. and Thorne, R.: Snowmelt contribution to discharge from a large mountainous catchment in subarctic Canada, Hydrol. Processes, 20, 2129–2139, 2006.

Woo, M. K., Thorne, R., Szeto, K., and Yang, D.: Streamflow hydrology in the boreal region under the influences of climate and human interference, Phil. Trans. R. Soc. B, 363(1501),

HESSD
7, 3129–3157, 2010

Uncertainty in the impacts of projected climate change

R. Thorne

2249–2258, doi:10.1098/rstv.2007.2197, 2008?.
Zhang, X., Vincent, L. A., Hogg, W. D., and Niitsoo, A.: Temperature and precipitation trends in Canada during the 20th century, Atmos. Ocean, 38, 395–429, 2000.

HESSD
7, 3129–3157, 2010

Uncertainty in the impacts of projected climate change

R. Thorne

Table 1. Calculated differences in average precipitation, evaporation and computed runoff from simulations using the baseline (1961 to 1990) and future scenarios (January 2040 to December 2069) for the Liard Basin.

Scenario	Average precipitation	Average evaporation	Average computed runoff	Scenario	Average precipitation	Average evaporation	Average computed runoff
Baseline	481 mm	104 mm	231 mm	Baseline	481 mm	104 mm	231 mm
CCCMA	18%	15%	15%	HadCM3 1 °C	5%	8%	4%
CSIRO	8%	12%	4%	HadCM3 2 °C	10%	15%	9%
HadCM3	13%	18%	10%	HadCM3 3 °C	15%	26%	12%
IPSL	6%	30%	(3)%	HadCM3 4 °C	21%	29%	18%
MPI	13%	22%	6%	HadCM3 5 °C	26%	36%	23%
NCAR	12%	15%	9%	HadCM3 6 °C	31%	42%	28%
HadGEM1	6%	20%	0%				

HESSD
7, 3129–3157, 2010

Table 2. Calculated differences in first day of prominent hydrograph rise and seasonal runoff from simulations using the baseline (1961 to 1990) and future scenarios (January 2040 to December 2069) for the Liard Basin. A positive number of days signify an earlier rise in the hydrograph rise.

Scenario	Date of hydrograph rise (days)	Winter runoff (%)	Spring runoff (%)	Summer runoff (%)	Autumn runoff (%)
CCCMA	3	7	24	9	18
CSIRO	1	3	16	(3)	10
HadCM3	3	5	25	2	13
IPSL	11	3	36	(22)	9
MPI	12	8	29	(11)	24
NCAR	4	5	21	2	12
HadGEM1	3	4	29	(11)	1
HadCM3 1 °C	1	1	11	0	7
HadCM3 2 °C	2	3	22	1	12
HadCM3 3 °C	4	3	22	1	12
HadCM3 4 °C	5	8	47	1	28
HadCM3 5 °C	6	13	62	0	37
HadCM3 6 °C	8	21	75	(1)	48

HESSD

7, 3129–3157, 2010

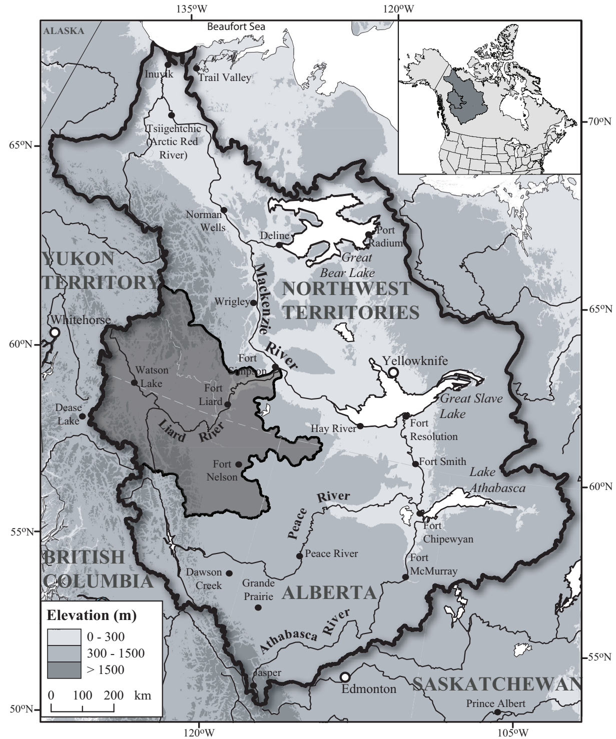

Fig. 1. Location of the Liard River in the Mackenzie River Basin.

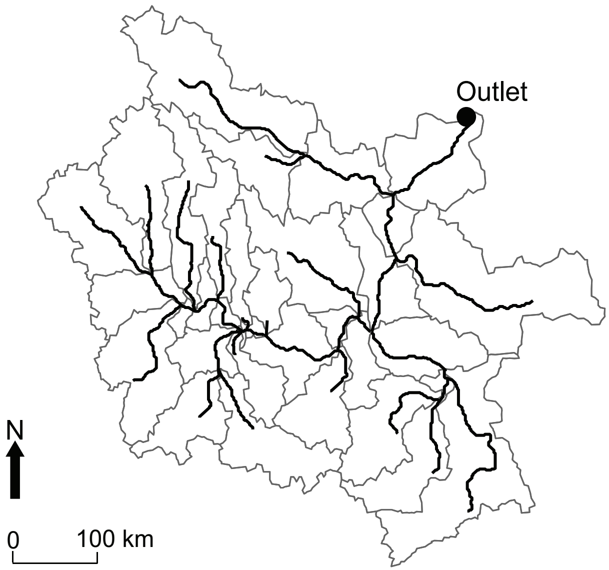

Fig. 2. Delineation of the Liard Basin into 35 ASAs, with the outlet of the basin occupying the 35th sub-basin.

Discussion Paper | Discussion Paper | Discussion Paper | Discussion Paper |

HESSD
7, 3129–3157, 2010

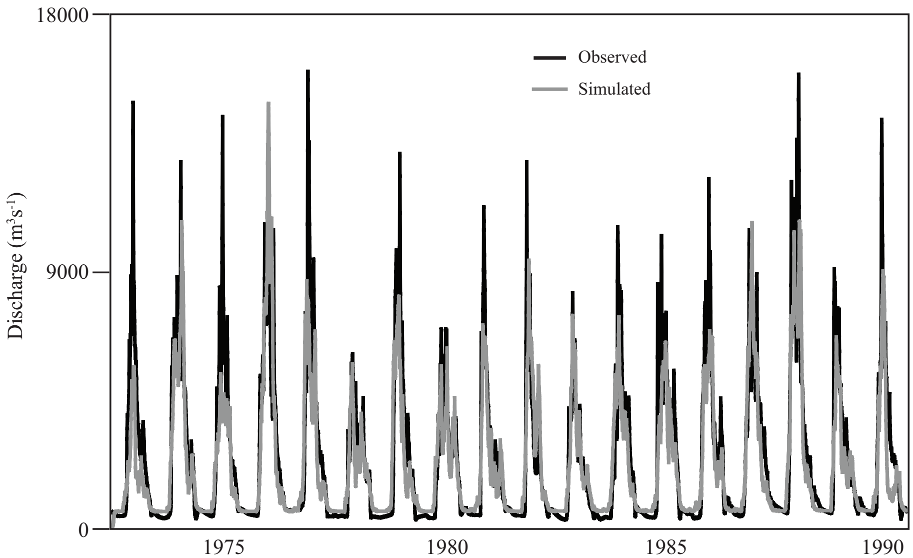

Fig. 3. Comparison of measured and simulated streamflow for the Liard River at its outlet near Fort Simpson from 1973 to 1990.

HESSD
7, 3129–3157, 2010

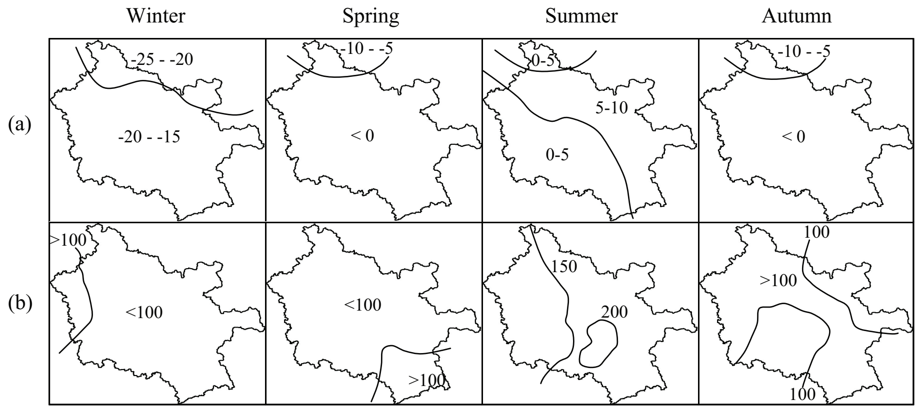

Fig. 4. Distribution of seasonal **(a)** temperature and **(b)** precipitation according to the CRU TS 3.0. The Liard Basin is outlined in black.

HESSD
7, 3129–3157, 2010

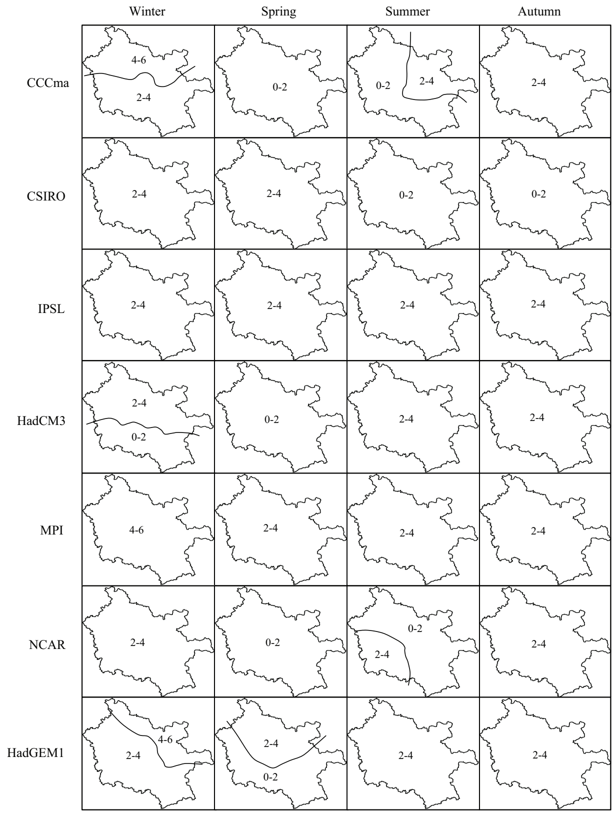

Fig. 5a. Distribution of seasonal changes in projected air temperatures under the 2˚C prescribed warming scenario for seven GCMs (2040–2069). The Liard Basin is outlined in black.

HESSD
7, 3129–3157, 2010

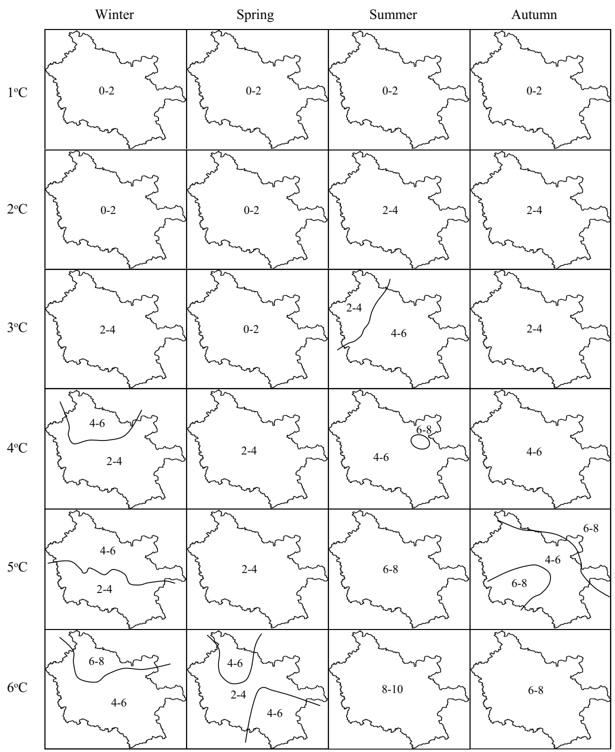

Fig. 5b. Distribution of seasonal changes in projected air temperature under prescribed increases of 1 to 6 °C in global mean air temperature by the UKMO HadCM3 GCM. The Liard Basin is outlined in black.

HESSD
7, 3129–3157, 2010

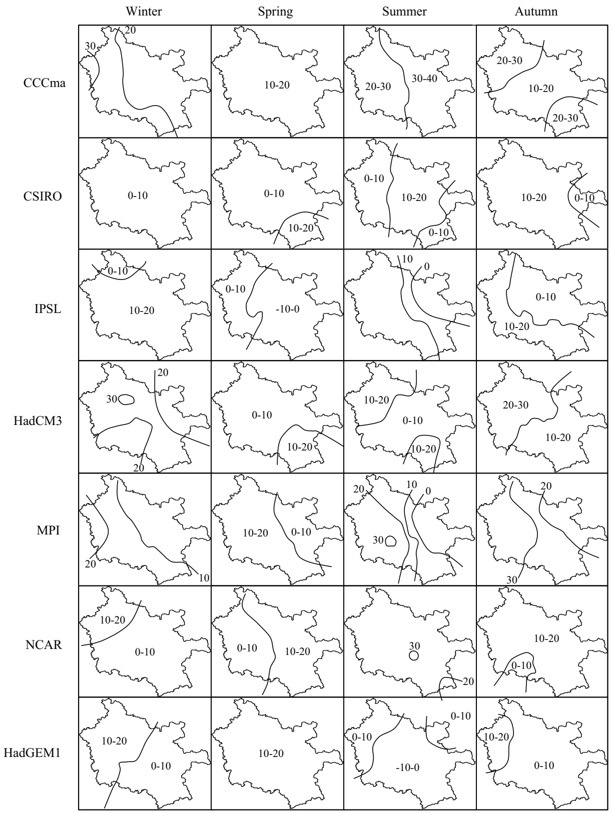

Fig. 6a. Distribution of seasonal changes in projected precipitation under the 2 °C prescribed warming scenario for seven GCMs (2040–2069). The Liard Basin is outlined in black.

HESSD
7, 3129–3157, 2010

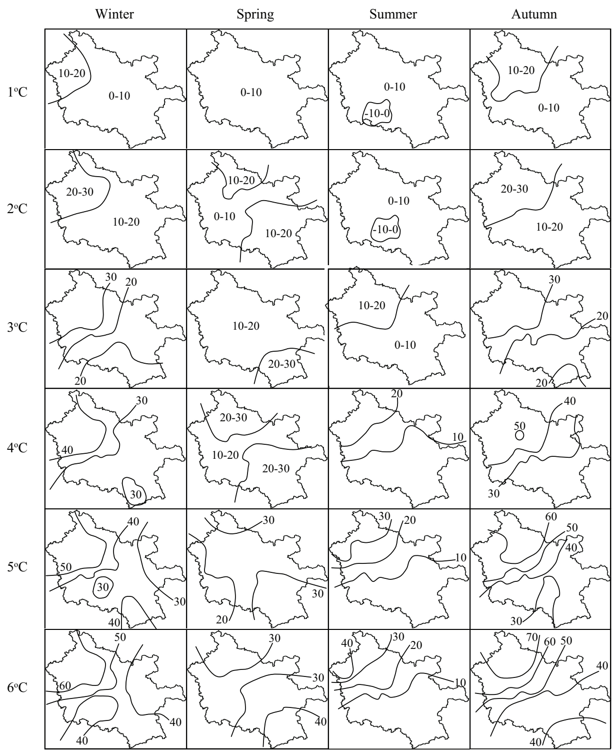

Fig. 6b. Distribution of seasonal changes in projected precipitation under prescribed increases of 1 to 6 °C in global mean air temperature by the UKMO HadCM3 GCM. The Liard Basin is outlined in black.

HESSD
7, 3129–3157, 2010

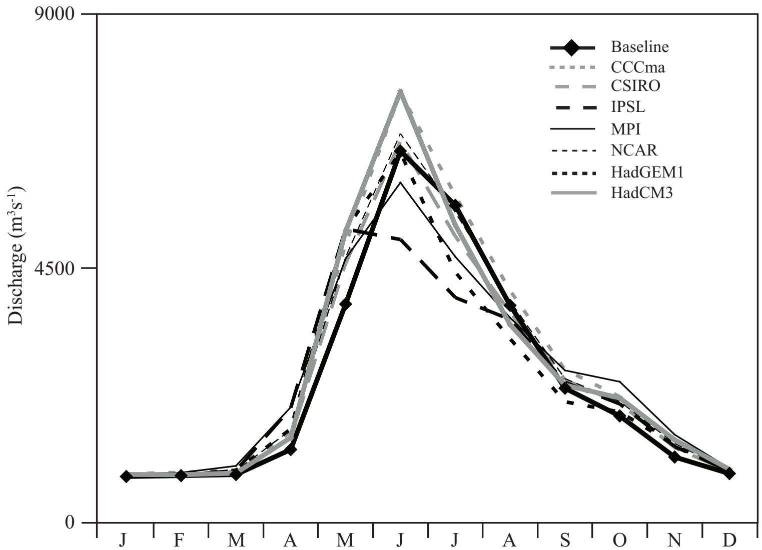

Fig. 7. Comparison of baseline and projected mean monthly river discharge under the 2 °C prescribed warming scenario for seven GCMs (2040–2069).

HESSD

7, 3129–3157, 2010

Uncertainty in the impacts of projected climate change

R. Thorne

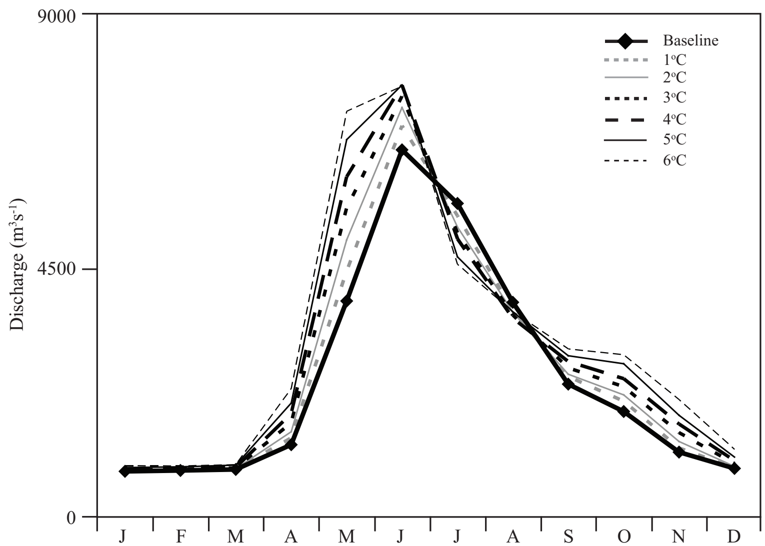

Fig. 8. Comparison of baseline and projected mean monthly river discharge under prescribed increases of 1 to 6 °C in global mean air temperature by HadCM3.

HESSD

7, 3129–3157, 2010

Uncertainty in the impacts of projected climate change

R. Thorne